EFFECT OF SODIUM LAURYL SULFATE (SLS)/CARBON NANOTUBES ON THE PROPERTIES OF CELLULOSE MEMBRANE ISOLATED FROM MAIZE STALK

N. JAFTA,[*] M.J. MOCHANE,[*] T.C. MOKHENA[**] and K. LEBELO[*]

[*]*Department of Life Sciences, Central University of Technology, Free State, Private Bag X20539, Bloemfontein, 9300, South Africa*
[**]*DSI Nanotechnology Innovation Centre, Advanced Materials Division, Mintek, Randburg, South Africa*

Received December 6, 2021

Composite systems made of a cellulose matrix reinforced with carbon nanotubes are promising materials for different applications, such as portable electronic and medical diagnostics devices. The properties of such systems are dependent on the dispersion of the carbon nanotubes within the nanocomposite product. This study reports on the fabrication and characterization of cellulose/carbon nanotubes (CNTs) composite membranes in the absence and presence of sodium lauryl sulfate (SLS) *via* the vacuum filtration process. SLS was used in order to improve the dispersion of CNTs. The nanocomposite membrane was prepared in three CNTs:cellulose ratios, *viz.* 1:1; 1:0.5; 1:0.3. The resulting membranes were analysed by means of SEM, transmission electron microscopy (TEM), X-ray diffraction (XRD), Fourier transform infrared spectroscopy (FTIR), and thermogravimetric analysis (TGA). SEM and TEM images showed that the presence of sodium lauryl sulfate (SLS) resulted in a better dispersion of the carbon nanotubes within the cellulose matrix with few visible agglomerates. The incorporation of CNTs in the absence of SLS resulted in superior thermal stability, when compared to SLS-based composite and neat cellulose membranes. The FTIR spectra of the membrane formed in the presence of SLS showed symmetric and asymmetric peaks for SLS, while, naturally, these peaks were absent in the membrane without SLS, which confirmed the presence of SLS in SWCNT.

Keywords: cellulose nanofibers, CNTs, composites membrane, sodium lauryl sulfate, maize stalk

INTRODUCTION

The current society is facing a lot of challenges with regard to plastic wastes and the crisis of energy, causing environmental concerns.[1] There is an urgent need to reduce the amount of plastic waste in order to decrease the adverse impact of petroleum-based plastics on the environment. The fabrication of sustainable and environmentally friendly materials has gained a huge interest in both the academic and industrial sectors.[2] The utilization of biodegradable materials provides a viable solution for reducing the amount of non-biodegradable polymers used, thus protecting the environment for future generations. Biomaterials feature unique advantages, such as biodegradation and renewability, hence reducing environmental pollution.[3] Cellulose is an abundant and biodegradable polymer that is produced from renewable resources.

Cellulose is employed in different applications, such as portable electronics, papermaking, textiles, biomedical materials, wood adhesives, food coatings, construction, and for wastewater treatment.[4-5] In most cases, various fillers (*viz.* graphene, carbon nanotubes and zinc oxide) are introduced into cellulose to improve its overall properties. Most of these fillers are chosen based on the intended application. This has resulted in cellulose composites with excellent conduction,[6] photoluminescent,[7] antimicrobial,[8] magnetic,[9] catalytic,[10] flame retardant and acoustic dampening[11] properties, which has further broadened the applications of cellulose.

Amongst the above-mentioned fillers, CNTs have been utilized as a reinforcement material for cellulose to produce multifunctional composite products for advanced applications, such as portable flexible electronics, semiconductors, and in biotechnology.[11-14] Pang *et al.*[11] prepared carbon nanotube/cellulose paper via vacuum filtration. The authors reported that the CNT/cellulose papers showed better properties, *i.e.*, electrical conductivity, electromagnetic interference (EMI), and electrochemical properties compared to the neat cellulose papers. Qi *et al.*[15] prepared carbon nanotube/cellulose composite aerogels for vapour sensing. The fabricated 3D porous structure

consisting of CNT and cellulose aerogels was found to provide efficient and direct contact with the vapours. Furthermore, this was reported to enhance a fast response, as well as electrical resistance change for vapours. Elsewhere in the literature, Gnanaseelan and co-workers[16] prepared cellulose/single walled carbon nanotubes (SWCNT) and cellulose/multiwalled carbon nanotubes (MWCNT) for thermoelectric materials, with CNTs in the concentration range of 2-10 wt%. It was reported that the composite system consisting of SWCNT showed higher electrical conductivity and Seebeck coefficient when compared with the MWCNTs based nanocomposites.

In most of the reported studies, the dispersion of CNTs within the cellulose matrix has been a challenge. For instance, Maria *et al.*[12] fabricated multiwalled CNT/cellulose composites by mixing both cellulose and multiwalled CNTs in a gelatin solution, followed by drying at room temperature. Gelatin was used as a dispersing agent for CNTs. CNTs were found to cover the surface of the cellulose fibers with some forming bridge-like structures. These interconnected bridge-like structures were formed by individual CNTs to create numerous electrical paths. Therefore, the presence of well-dispersed CNTs significantly improved the electrical properties and thermal stabilities of cellulose.

In this study, single-walled carbon nanotubes (SWCNTs), in the absence or presence sodium lauryl sulfate (SLS), were incorporated into cellulose to fabricate membrane composites through the vacuum filtration process. Dispersants are usually introduced into the suspension of conductive fillers in order to retain their dispersed state during preparation, and thus enhance their dispersion within the nanocomposite materials. The conductive fillers in an aqueous medium have the tendency of agglomerating because the van der Waals attraction is higher than the electrostatic repulsion. Herein, SLS was added into the carbon nanotubes suspension as a dispersant in order to enhance the steric hindrance and the electrostatic stabilization between the nanoparticles. The as-prepared CNTs suspension was then added into the cellulose suspension to yield nanocomposite materials. The effect of CNTs on the properties of cellulose was examined using TGA, SEM, TEM and XRD. The cellulose/CNT membrane composites were fabricated using various cellulose:CNT ratios, *i.e.*, of 1:1; 1:0.5; and 1:0.3. Nanocellulose was extracted from maize stalk, which was sourced as agricultural waste to create the cellulose/SWCNTs membrane. The aim of the research was to investigate the effect of SWCNT and SWCNT/SLS on the properties of the cellulose matrix, such as morphology, thermal stability and crystallinity. To our knowledge, there are limited studies on the fabrication of cellulose/carbon nanotubes membranes using SLS as a dispersing agent.

EXPERIMENTAL

Materials

Maize stalks were provided by a local farmer in Cofimvaba in Eastern Cape, South Africa. Sodium hydroxide (NaOH) was supplied in pellet form by Sigma-Aldrich, South Africa. It was a chemically pure (CP) grade with an assay of 99%, and a density of 2.13 g cm^{-3}. Sodium lauryl sulphate (SLS) (90% assay) was supplied in powder form by Merck, South Africa. It has a density of 1.01 g cm^{-3} and its chemical formula is $CH_3(CH_2)_{11}OSO_3Na$. It was used as an emulsifier. Sodium chlorite ($NaClO_2$), with the purity of 80% and density of 2.5 g cm^{-3}, was procured from Sigma Aldrich, South Africa. Potassium hydroxide (KOH) was supplied in pellet form by Sigma-Aldrich, South Africa. It was a chemically pure (CP) grade with an assay of 99%, and a density of 2.12 g cm^{-3}. Single-walled carbon nanotubes (SWCNTs) were supplied by OCSiAl, Luxembourg (density of 1.35 g/cm^3, purity of 75% and metal impurities of 15%; with a diameter below 2 nm and length of >1 micron).

Preparation of cellulose nanofibrils (CNFs)

Maize stalks were ground into a coarse powder using a Hamermeul, and then dried in a vacuum oven at 60 °C for 24 hours. The dried maize stalk powder was weighed and treated with 1.5% NaOH, 1.5% $NaClO_2$, and 1.5% KOH, respectively, at 80 °C for an hour. Each treatment was repeated four times, with repeated washes using deionized water until a neutral pH was achieved. The powder content during all these chemical treatments was kept in the range of 5-6 wt%. After these treatments, the resulting powder was oven dried at 40 °C for 24 hours. The obtained powder (2 wt%) was agitated with a blender, then subjected to mechanical grinding using a Supermass Colloider (MKCA-39Masuko Sangyo Co, Ltd., Japan) at 1500 rpm for 25 minutes, *viz.* until a gel-like substance was obtained. The obtained cellulose nanofibril suspensions were sonicated for 5 minutes at 80% amplitude and agitated with a mechanical blender.

Preparation of membranes

Composite membranes were prepared in three different ratios. CNTs were added into the cellulose suspension, with cellulose:SWCNT ratios of 1:1; 1:0.5 and 1:0.3. The obtained suspension was then sonicated at 80% amplitude for 5 minutes, followed by mechanical agitation using a blender. The mixture was then poured onto a filtration funnel, fitted with a commercial membrane (PLAC07610) (PLA). After filtration, the wet cellulose composite was peeled off and pressed for 72 hours at room temperature. In the case of SLS-based composites, 0.5 g of SLS was mixed with CNTs in deionized water. The obtained mixture was then introduced into the cellulose suspension, followed by the vacuum filtration process. For comparison, the cellulose suspension was also sonicated and agitated with a blender, then filtered and pressed to obtain a neat cellulose membrane.

Characterization

Scanning electron microscopy

A Shimadzu ZU SSX-550 Superscan scanning electron microscope (SEM) was used to identify the morphological changes of the fractured membranes in the presence of CNT and SLS. The analysis of the samples was carried out on fractured specimens using liquid nitrogen. The samples were coated with gold before the SEM analysis.

Transmission electron microscopy

A Philips CM 200 transmission electron microscope (TEM), equipped with an AMT XR-60 CCD digital camera system, was employed to determine the dispersion of the CNTs within the membranes. An accelerating voltage of 80 kV was used for the TEM analysis.

XRD analysis

The X-ray diffraction profiles of the cellulose and its composite membranes were measured using a Bruker AXS X-ray diffractometer D8 Advance, equipped with position sensitive Vantec-1 detector and CuKα radiation ($\lambda K\alpha_1$ = 1.5406 Å). The crystallinity indices (*CI*) of the cellulose and its composites were determined as the height ratio between the intensity of the crystalline peak (I_{002} - I_{am}) and total intensity (I_{002}) from the XRD diffractogram (Eq. 1):

$$CI = \frac{[I_{200} - I_{am}]}{I_{200}} x\ 100\% \qquad (1)$$

where *CI* is the degree of crystallinity, I_{002} is the crystalline peak and I_{am} is the amorphous state.

Chemical analysis

The spectra of cellulose and its composites were obtained by attenuated total reflectance-Fourier transform infrared spectroscopy (ATR-FTIR) using a Perkin-Elmer Spectrum 100. The samples were scanned between 400-4000 cm^{-1}, at a resolution of 4 cm^{-1}.

Thermogravimetric analysis (TGA)

Thermogravimetric analysis was carried out with a Perkin Elmer TGA7 thermogravimetric analyser, at a heating rate of 10 °C min^{-1} and purged with nitrogen as purge gas. Approximately 5 to 10 mg of sample was heated from 30 to 600 °C and the sample's weight loss was recorded.

RESULTS AND DISCUSSION

Microscopic analysis

Figure 1 presents the SEM images of the cellulose and composite membranes. The neat cellulose membrane shows a typical web-like structure (Fig. 1a). There are clear bright spots on the surface of the cellulose/SWCNT membrane (Fig. 1b), as noted by symbols A, B and C, which may be attributed to a slight but observable agglomeration of the SWCNTs. Similarly, Maria *et al.*[12] observed that the MWCNTs were covering the surface of the cellulose fibres, with some carbon nanotubes forming bridge-like structures. In the presence sodium lauryl sulfate (SLS), the resulting nanocomposite became more compact, with no visible bright spots (Fig. 1c). This could probably be due to improved dispersion of the SWCNTs in the presence of SLS.

In Figure 2a, it can be seen that the SWCNTs were agglomerated in the absence of SLS (see symbol A in Fig. 2a). On the contrary, the presence of SLS improved the dispersion of the CNTs (see symbol C in Fig. 2b). In the absence of SLS, there is strong affinity between the nanoparticles, which leads to agglomeration. Conductive nanoparticles are likely to adhere to each other upon direct interaction due to forces such as electrostatic, magnetic and van der Waals forces.[17] Therefore, carbon nanotubes, due to their high aspect ratio and flexibility, have a huge possibility to form clusters, in the

absence of a dispersing agent.[18] It seems that SLS was able to eradicate the surface interaction between the SWCNTs, which was also evident by a smaller average particle size of the carbon nanotubes in the presence of SLS, *i.e.*, 14.8 nm, when compared with non-modified carbon nanotubes (*viz*. 19 nm). Surfactants have the ability of dispersing CNTs in aqueous solution through the hydrophobic/hydrophilic process. In this process, the hydrophobic tail of the surfactant adsorbs CNTs, whereas the hydrophilic head interacts with the water.[19]

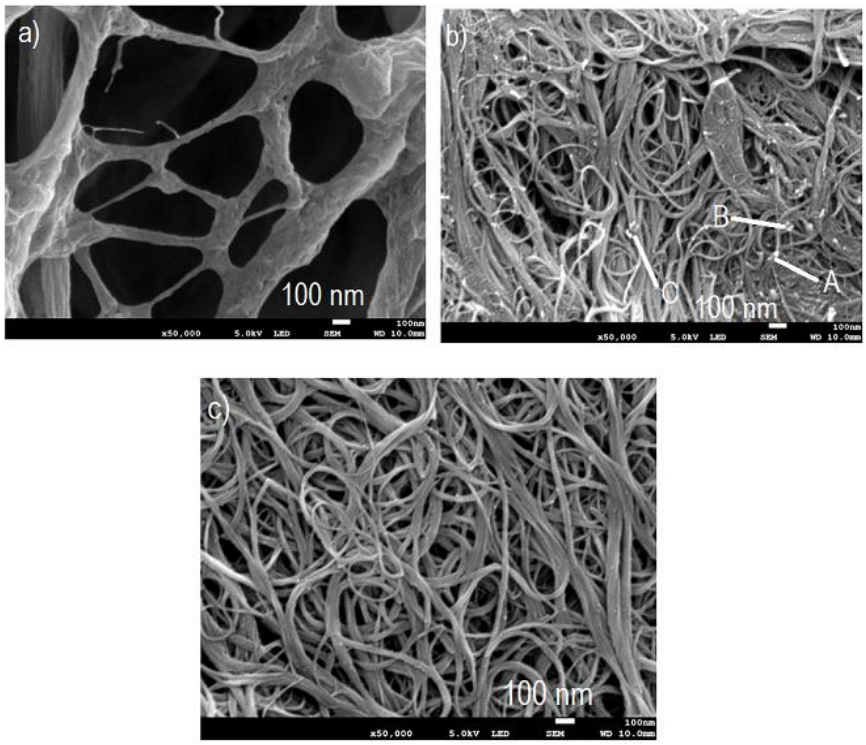

Figure 1: SEM images of (a) cellulose, b) cellulose:SWCNT 1:0.5 (SWCNT) composite, and (c) cellulose:SWCNT:SLS 1:0.5:1 composite

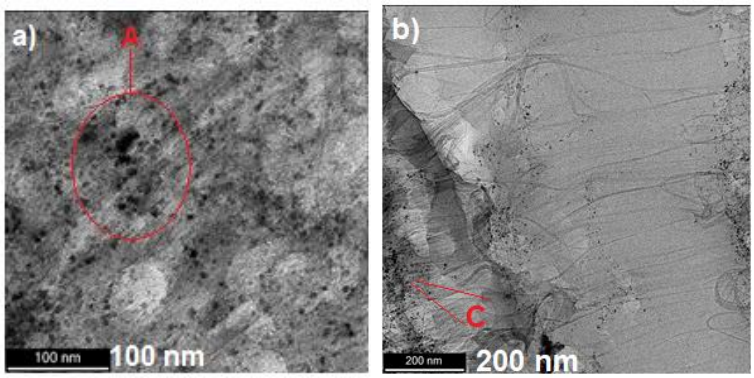

Figure 2: TEM images of (a) cellulose:SWCNT 1:0.5 and (b) cellulose:SWCNT:SLS 1:0.5:1

XRD analysis

Figures 3-4 show the XRD diffractograms of cellulose membranes, cellulose/SWCNTs and SWCNT-SLS/cellulose membrane composites. In Figure 3, all the cellulose-based composites exhibit peaks at 2θ = 14.9º, 16.0º and 23.4º, corresponding to the characteristic peaks of cellulose I.[20] The small peak shoulders around 2θ = 14.9° and 16.0° correspond to the 110 and 110 diffraction planes in the cellulose, while the 23.4° and 35.0° peaks correspond to the 200 and 004 planes, respectively.[21,22] The incorporation of SWCNT, with or without SLS, produced no significant changes in the diffraction peaks, when compared to the neat cellulose membrane (see Fig. 3). However, there was a reduction in the intensity of the peaks with the addition SWCNTs, which may be due to the presence of CNTs between the fibrils. The presence of these CNTs may hinder the strong cohesion between the fibrils

through hydrogen bonding, resulting in a decrease in the crystallinity of the composite (Figs. 3 and 4). The decrease in crystallinity is evident from Table 1. The presence of SLS resulted in a further reduction in the crystallinity index, when compared with the non-modified SWCNT-based composites. This may be ascribed to the small-sized CNTs being able to enter between the fibrils and the SLS coating of cellulose, thus further inhibiting the formation of the interfibril hydrogen bonding network between the fibrils (Figs. 3 and 4), as a result decreasing the crystallinity. It seems as if at low CNTs content, the CNTs are able to remain on the surface of the fibrils, which in turn, impedes the formation of hydrogen bonds between the fibrils. This results in a reduction of crystallinity, which is dependent on the number of hydrogen bond sites within cellulose composites. In the case of the neat cellulose-based membrane, there is a large number of hydroxyl groups on the surface of the fibrils available for formation of hydrogen bonds, however, the presence of CNTs may cover some of the functionalities, which results in reducing the overall crystallinity and/or impeded interfibril interaction. This is confirmed by a significant decrease at higher CNTs content, *i.e.* >10% for Cellulose:CNT 1:1 and Cellulose:CNT:SLS 1:1:1. This clearly indicates that more CNTs were situated on the surface of the cellulose fibrils, thus inhibiting strong adhesion between the fibrils. It seems that CNTs served as a link between the fibrils rather than the original hydrogen bonds. The membranes that contained CNTs were smooth and easily peeled-off from the filter after the drying process, when compared to the neat cellulose-based membranes, which were rougher and more difficult to peel-off from the filter after drying. The in-plane regularity at 100 for carbon nanotubes appears at 45°,[23] as seen from Figure 3 and Figure 4.

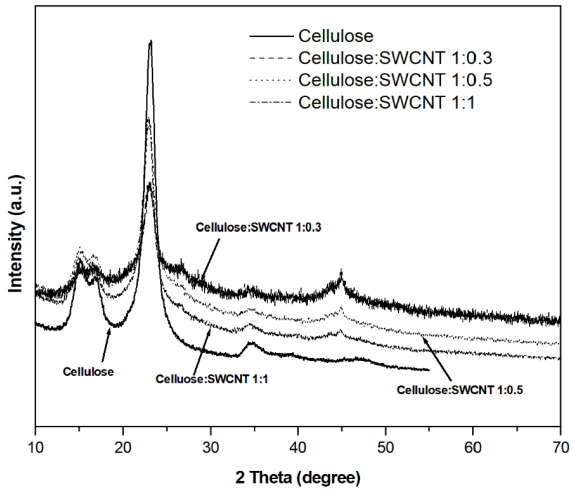

Figure 3: XRD patterns of cellulose, cellulose:SWCNT 1:0.3 and cellulose:SWCNT 1:0.5 and cellulose:SWCNT 1:1

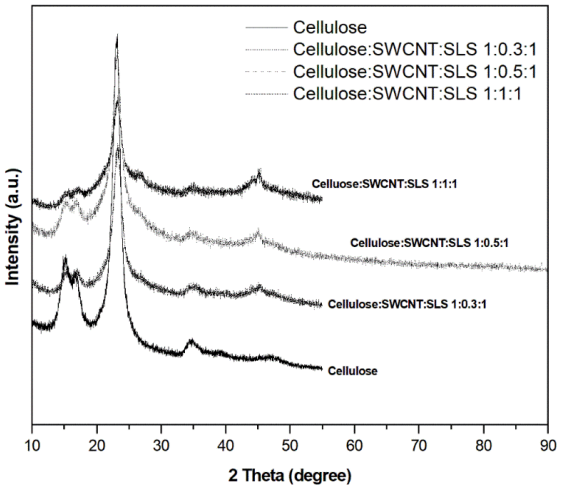

Figure 4: XRD patterns of cellulose, cellulose:SWCNT: 1:0.3:1, cellulose:SWCNT:SLS 1:0.5:1 and cellulose:SWCNT:SLS 1:1:1

Table 1
Crystallinity index for the cellulose membrane and its SWCNT/cellulose composites

Membrane	Crystallinity index CI (%)
Pure cellulose	71.5
Cellulose:SWCNT 1:0.3	67.1
Cellulose:SWCNT 1:0.5	63.8
Cellulose:SWCNT 1:1	59.2
Cellulose:SWCNT:SLS 1:0.3:1	65.8
Cellulose:SWCNT:SLS 1:0.5:1	62.0
Cellulose:SWCNT:SLS 1:1:1	59.4

Fourier-transform infrared (FTIR) spectroscopy

Figures 5 and 6 illustrate the FTIR spectra of the neat cellulose membrane, cellulose/SWCNT composites and SWCNT-SLS/cellulose membrane composites. The absorption bands of cellulose-based materials are normally reported in two wavenumber ranges, *i.e.* 3500-2800 cm^{-1} and 1650-500 cm^{-1}. The detected peaks in the wavenumber range of 3334-2896 cm^{-1} are typical of polysaccharide stretching vibrations of O-H and C-H bonds.[24-26] In this study, the spectrum of the neat cellulose in Figure 5 shows a stretching vibration of the hydroxyl group in polysaccharides, which is characterized by a large peak at 3334 cm^{-1}. According to the literature, this peak also comprises the inter- and intramolecular hydrogen bond vibrations.[26] The CH stretching vibration of all hydrocarbon constituents in polysaccharides is linked to the band at 2896 cm^{-1} for neat cellulose.[23,24] Stretching and bending vibrations of $-CH_2$ and -CH, -OH and C-O bonds in cellulose are represented by the absorption bands at 1423, 1356, 1312, 1154, 1104, 1021 cm^{-1} and 894 cm^{-1}.[24,27,28] The band at roughly 1423-1430 cm^{-1} is related to the crystalline structure of cellulose, while the band at 894 cm^{-1} is ascribed to the amorphous area of cellulose.[29,30]

The functional groups of carbon nanotubes, which are located at the wavenumbers 3323 cm^{-1} and 1034 cm^{-1}, are attributed to -OH and C-O stretching, respectively. However, in the cellulose/SWCNTs composites, the -OH and C-O stretching of CNTs overlap with those of the cellulose, which occur at 3334 cm^{-1} (-OH) and 1024 cm^{-1} (C-O). The addition of CNTs seems to have little effect on the peaks of cellulose, compared to the neat sample. The peak around 1641 cm^{-1} for cellulose is attributed to the absorption of water in the cellulose (Symbol A).

Figure 7 illustrates the FTIR spectra of cellulose and cellulose:CNT:SLS membranes at various ratios of CNT and SLS. The presence of SLS with the chemical structure ($C_{12}H_{25}NaO_4S$) in the composites is proved by symmetric stretching at 2843 cm^{-1} and asymmetric stretching at 2910 cm^{-1} (as shown by symbol B in Fig. 7). The asymmetric and symmetric peaks seem to be absent in the non-SLS peaks, as shown by symbol C in Figure 8. Furthermore, as observed from the absorption bands associated with cellulose, it is also clear that the addition of SLS to the SWCNTs resulted in the absorption bands becoming less discernible, when compared with non SLS-based composites, as shown in Figure 8 by symbol D. There is no clear explanation for such a behavior.

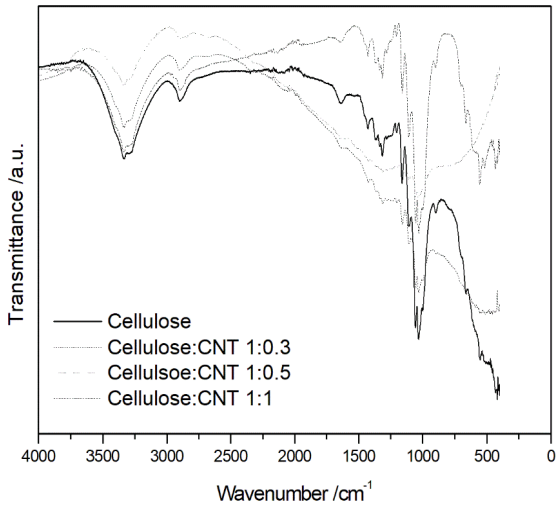

Figure 5: FTIR spectra of cellulose, cellulose:SWCNT 1:0.3 and cellulose:SWCNT 1:0.5 and cellulose:SWCNT 1:1

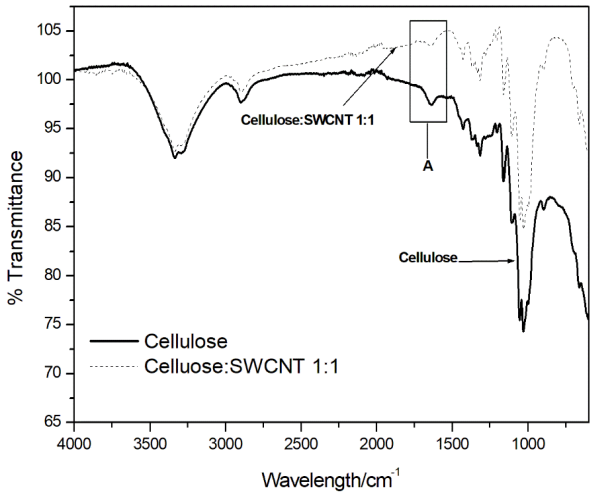

Figure 6: FTIR spectra of cellulose and cellulose:SWCNT 1:1

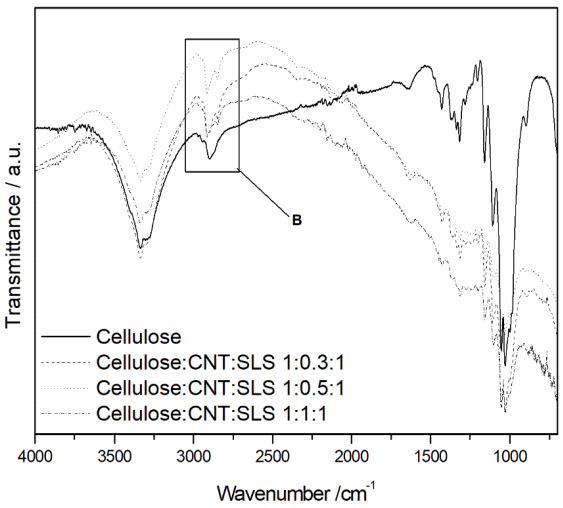

Figure 7: FTIR spectra of cellulose, cellulose:SWCNT:SLS 1:0.3:1, cellulose:SWCNT:SLS 1:0.5:1 and cellulose:SWCNT:SLS 1:1:1

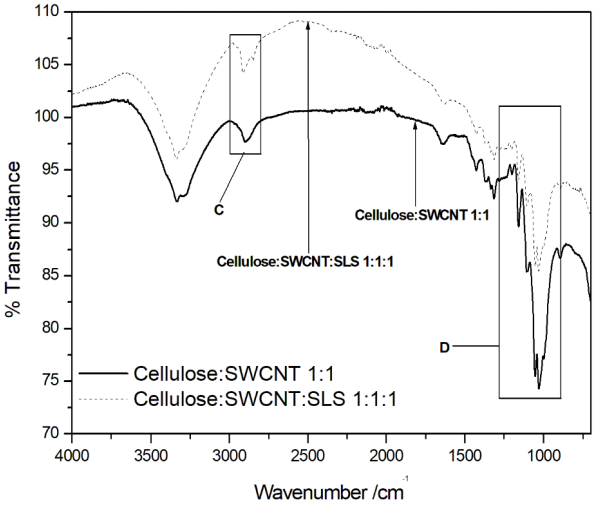

Figure 8: FTIR spectra of cellulose, cellulose:SWCNT 1:1, cellulose:SWCNT:SLS 1:1:1

Thermogravimetric analysis

Figures 9-12 depict the TGA curves of cellulose and its composites. All the samples exhibited two degradation steps (Fig. 9). The first degradation step between 40 and 130 ℃ is ascribed to the evaporation of the absorbed water by cellulose, low molar mass components and volatile materials. The second degradation step between 200 and 400 ℃ is attributed to the degradation of the cellulose membranes. According to the literature,[31-34] the degradation of cellulose below 300 ℃ is known to take place faster because hydrogen bonds are being destroyed. Cellulose degradation between 300 and 390 ℃ produces products, such as ash, tar, condensable and non-condensable gases.

The addition of CNTs into the cellulose enhanced the thermal stability, as can be seen in Table 2 and Figure 9. For example, for neat cellulose, the $T_{10\%}$ (temperature of 10 degradation) was found to be 242.1 ℃, while for cellulose:SWCNT (1:0.3), the $T_{10\%}$ value was found to be 313 ℃, which is higher even than that of cellulose:SWCNT (1:1) (*viz.* 306.0 ℃). Similarly, for the carbon nanotube-based cellulose composites, $T_{40\%}$ was recorded at higher temperature when compared to the neat cellulose. The enhancement in thermal stability is due to the carbon nanotubes forming a physical heat barrier against the diffusion of the volatile products out of the system, which are produced during thermal decomposition, as a result enhancing the thermal stability. The heat barrier formed by the carbon nanotubes is capable of preventing the decomposition products diffuse out of the cellulose/SWCNTs system, as well as the penetration of heat into the system, thus, enhancing the thermal stability. Similar behavior has been reported in the literature.[31-34] The thermal stability of poly(ethylene 2,6-naphthalate)/CNT and poly(ethylene terephthalate)/CNT) nanocomposites has been investigated in previous studies.[31-32] It was reported that the addition of unmodified and modified carbon nanotubes to poly(ethylene 2,6-naphthalate) enhanced the thermal stability of the polymer matrix, which was attributed to the formation of a heat barrier by the CNTs.[31] Furthermore, the carbon nanotubes, which were modified with concentrated sulphuric acid and nitric acid to introduce the carboxylic acid into the surface of the nanotubes, enhanced the thermal stability even more due to better interfacial adhesion between the polymer and the carbon nanotubes.

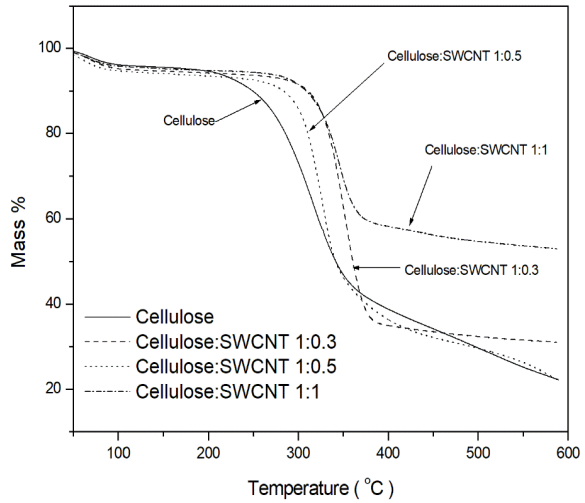

Figure 9: TGA curves of cellulose, cellulose:SWCNT 1:0.3, cellulose:SWCNT 1:0.5 and cellulose:SWCNT 1:1

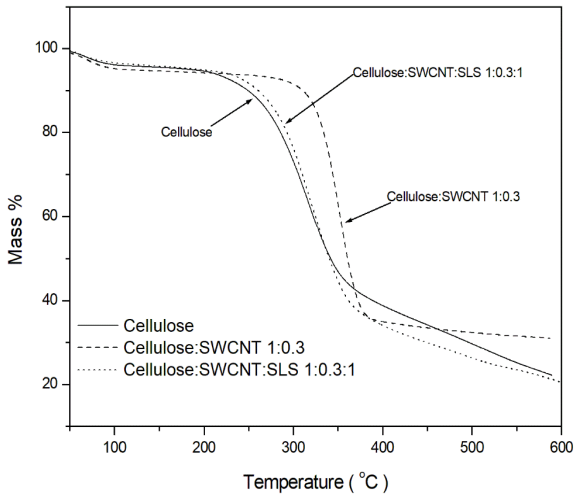

Figure 10: TGA curves of cellulose, cellulose:SWCNT 1:0.3 and cellulose:SWCNT:SLS 1:0.3:1

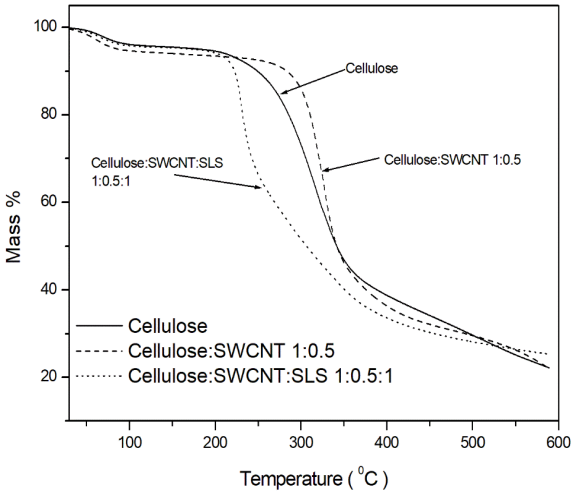

Figure 11: TGA curves of cellulose, cellulose:SWCNT 1:0.5, and cellulose:SWCNT:SLS 1:0.5:1

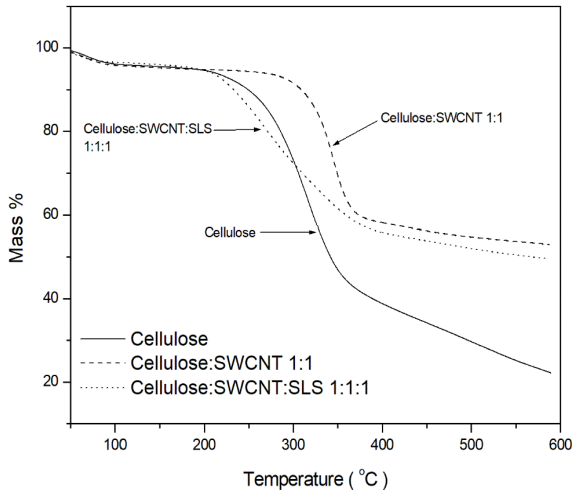

Figure 12: TGA curves of cellulose, cellulose:SWCNT 1:1, and cellulose:SWCNT:SLS 1:1:1

Table 2
Degradation temperatures at 10 and 40% for cellulose membranes

Samples	$T_{10\%}$	$T_{40\%}$
Cellulose	242.1	319.7
Cellulose:SWCNT (1:0.3)	313.9	353.2
Cellulose:SWCNT (1:0.5)	276.5	329.5
Cellulose:SWCNT (1:1)	306.0	372.7
Cellulose:SWCNT:SLS (1:0.3:1)	264.8	323.6
Cellulose:SWCNT:SLS (1:0.5:1)	221.7	270.6
Cellulose:SWCNT:SLS (1:1:1)	231.0	356.7

$T_{10\%}$ and $T_{40\%}$ denote the temperatures of 10 and 50% degradation, respectively

Figures 10-12 illustrate the thermal stability of the neat cellulose membrane and SLS modified CNT based cellulose membranes. The addition of SLS reduced the thermal stability of the modified SWCNT/cellulose composites in all the investigated samples when compared with the unmodified composites. For example, the $T_{10\%}$ for cellulose:SWCNT:SLS (1:0.3:1) showed 15.6% reduction, when compared with that of cellulose:SWCNT (1:0.3), while the $T_{40\%}$ for cellulose:SWCNT:SLS (1:0.3:1) revealed 8.4% reduction in relation to the unmodified cellulose:SWCNT (1:0.3). It seems

that the presence of sodium lauryl sulfate might have initiated the degradation of the entire composite, considering the low degradation temperature of surfactants – in the range from 200 to 300 ℃. The presence of a lower thermally stable material in the form of SLS accelerated the degradation of the composites and, as a result, reduced the thermal stability. On the contrary, Sefadi and co-workers[35] reported an increase in the thermal stability of graphite modified sodium dodecyl sulfate (SDS) reinforced ethylene vinyl acetate (EVA). This behavior was attributed to a strong interaction between the free radical chains of the polymer and volatile products with the filler. This strong interaction retarded the degradation of the polymer, as well as the diffusion of the volatile materials out of the composite system, as a result improving the thermal stability.

CONCLUSION

The study provides an insight into the fabrication of non-SLS SWCNT/cellulose and SLS/SWCNT/cellulose composites for advanced applications. The effect of SLS and SWCNT, as well as the content of SWCNT, on the properties of the cellulose matrix and the resulting composites has been reported in this study. TEM and SEM showed better dispersion of carbon nanotubes in the cellulose matrix in the presence of SLS. In the absence of SLS, there were clear agglomerates of the carbon nanotubes on the surface of the cellulose fibrils.

The presence of carbon nanotubes in the cellulose matrix enhanced the thermal stability of the composites, meanwhile the addition of SLS to the cellulose/SWCNT decreased the thermal stability. In light of the findings, it can be concluded that the presence of SWCNT, without SLS, was able to act as a heat barrier, blocking the volatiles within the system, while also preventing the entrance of heat into the system. The incorporation of SWCNT and its modification with SLS seems to cause little or no changes in the peak positions associated with cellulose-based materials. However, there was a reduction in the intensity of the crystal lattice peaks with the addition SWCNTs, which may suggest that SWCNTs were able to enter in between the fibrils and decrease the number of hydrogen bonds within the composite system, thus there was a decrease in the crystallinity at the higher SWCNT content.

ACKNOWLEDGMENTS: The National Research Foundation (NRF) of South Africa is acknowledged for financial support (Grant numbers 127278 and 129347).

REFERENCES

[1] J. K. Debrah, D. G. Vidal and M. A. P. Dinis, *Urban Sci*., **5**, 12 (2021), https://doi.org/10.3390/urbansci5010012

[2] G. K. Gupta and P. Shukla, *Front. Chem*., **8**, 601256 (2020), https://doi.org/10.3389/fchem.2020.601256

[3] A. A. Singh, M. E. Genovese, G. Mancini, L. Marini and A. Anthanassiou, *ACS Sustain. Chem. Eng*., **8**, 4128 (2020), https://doi.org/10.1021/acssuschemeng.9b06760

[4] D. Trache, A. F. Tarchoun, M. Derradji, T. S. Hamidon, N. Masruchin *et al*., *Front. Chem*., **8**, 392 (2020), https://doi.org/10.3389/fchem.2020.00392

[5] R. J. Moon, G. T. Schueneman and J. Simonsen, *JOM*, **68**, 2383 (2016), https://doi.org/10.1007/s11837-016-2018-7

[6] L. Jabbour, D. Chaussy, B. Eyraud and D. Beneventi, *Compos. Sci. Tech*., **72**, 616 (2012), https://doi.org/10.1016/j.compscitech.2012.01.006

[7] P. Sarrazin, L. Valecce, D. Beneventi, D. Chaussy, L. Vurth *et al*., *Adv. Mater*., **19**, 3291 (2007), https://doi.org/10.1002/adma.200700814

[8] L. Qian, Y. Guan, Z. Ziaee, B. He, A. Zheng *et al*., *Cellulose*, **16**, 309 (2009), https://doi.org/10.1007/s10570-008-9270-0

[9] A. C. Small and J. H. Johnston, *J. Colloid. Int. Sci*., **331**, 122 (2009), https://doi.org/10.1016/j.jcis.2008.11.038

[10] S. Fukahori, Y. Iguchi, H. Ichiura, T. Kitaoka, H. Tanaka *et al*., *Chemosphere*, **66**, 2136 (2007), https://doi.org/10.1016/j.chemosphere.2006.09.022

[11] Z. Pang, X. Sun, X. Wu, Y. Nie, Z. Liu *et al*., *Vacuum*, **122**, 135 (2015), https://doi.org/10.1016/j.vacuum.2015.09.020

[12] K. H. Maria and T. Mieno, *J. Nanomat*., **2017**, 6745029 (2017), https://doi.org/10.1155/2017/6745029

[13] C. Chen, X. Bu, Q. Feng and D. Li, *Polymers*, **10**, 1000 (2018), https://doi.org/10.3390/polym10091000

[14] S. Palanisamy, V. Velusamy, S. Balu, S. Velmurugan, T. C. K. Yang *et al*., *Ultrason. Sonochem*., **63**, 104917 (2020), https://doi.org/10.1016/j.ultsonch.2019.104917

[15] H. Qi, J. Liu, J. Pionteck, P. Pötschke and E. Mäder, *Sens. Actuat. B Chem.*, **213**, 20 (2015), https://doi.org/10.1016/j.snb.2015.02.067
[16] M. Gnanaseelan, Y. Chen, J. Luo, B. Krause, J. Pionteck *et al.*, *Compos. Sci. Tech.*, **163**, 133 (2018), https://doi.org/10.1016/j.compscitech.2018.04.026
[17] S. Kawashima, J.-W. Seo, D. Corr, M. C. Hersam and S. P. Shah, *Mater. Struct.*, **47**, 1011 (2014), http://doi.org/ 10.1617/s11527-013-0110-9
[18] L. Vaisman, D. Wagner, and G. Marom, *Adv. Colloid, Int. Surf. Sci.*, **128–130**, 37(2006), http://dx.doi.org/10.1016/j.cis.2006.11.007
[19] W. H. Duan, Q. Wang and F. Collins, *Chem. Sci.*, **2**, 1407 (2011), https://doi.org/10.1039/C0SC00616E
[20] S. M. Mohomane, S. V. Motloung, L. F. Koao and T. E. Motaung, *Wood Res.*, **66**, 85 (2021), https://doi.org/10.37763/wr.1336-4561/66.1.8594
[21] M. Poletto, H. L. Ornaghi and A. J. Zattera, *Materials*, **7**, 6105 (2014), https://doi.org/10.3390/ma7096105
[22] Z. Tang, W. Li, X. Lin, H. Xiao, Q. Miao *et al.*, *Polymers*, **9**, 421 (2017), http://dx.doi.org/10.3390/polym9090421
[23] R. Das, M. E. Ali, S. B. A. Hamid, M. S. M. Annuar and S. Ramakrishma, *J. Nanomater.*, **2014**, ID 945172 (2014), https://doi.org/10.1155/2014/945172
[24] V. Hospodarova, E. Singovszka and N. Stevulova, *Am. J. Anal. Chem.*, **9**, 303 (2018), https://doi.org/10.4236/ajac.2018.96023
[25] M. Poletto, V. Pistor, M. Zeni and A. J. Zattera, *Polym. Degrad. Stab.*, **96**, 679 (2011), https://doi.org/10.1016/j.polymdegradstab.2010.12.007
[26] M. C. Popescu, C. M. Popescu, G. Lisa and Z. Sakata, *J. Mol. Struct.*, **988**, 65 (2011), https://doi.org/10.101/j.molstruc.2010.12.004
[27] F. Xu, J. Yu, T. Tesso, F. Dowell and D. Wang, *Appl. Energ.*, **104**, 801 (2013), https://doi.org/10.1016/j.apenergy.2012.12.019
[28] K. Fackler, J. S. Stevanic, T. Ters, B. Hinterstoisser, M. Schwanninger *et al.*, *Holzforschung*, **65**, 411 (2011), https://doi.org/10.1515/hf.2011.048
[29] M. Poletto, H. L. Ornaghi Júnior and A. J. Zattera, *Materials*, **7**, 6105 (2014), https://doi.org/10.3390/ma7096105
[30] M. Poletto, V. Pistor, R. M. C. Santana and A. J. Zattera, *Mater. Res.*, **15**, 421 (2012), https://doi.org/10.1590/S1516-14392012005000048
[31] J. Y. Kim, S. I. Han and S. Hong, *Polymer*, **49**, 3335 (2008), https://doi.org/10.1016/j.polymer.2008.05.024
[32] B. A. Alshammari and A. Wilkinson, *Appl. Petrochem. Res.*, **6**, 257 (2016), https://doi.org/10.1007/s13203-016-0161-2
[33] D. Bikiaris, *Materials*, **3**, 2884 (2010), https://doi.org/10.3390/ma3042884
[34] Y.-J. Choi, S.-H. Hwang, Y. S. Hong, J.-Y. Kim, C.-Y. Ok *et al.*, *Polym. Bull.*, **53**, 393 (2005), https://doi.org/10.1007/s00289-005-0348-7
[35] J. S. Sefadi, A. S. Luyt, J. Pionteck, F. Piana and U. Gohs, *J. Appl. Polym. Sci.*, **132**, 42396 (2015), https://doi.org/10.1002/app.42396